Ab Initio Deconstruction of the Vibrational Relaxation Pathways of Dilute HOD in Ice Ih

Hanchao Liu, Yimin Wang, and Joel M. Bowman*

Cherry L. Emerson Center for Scientific Computation and Department of Chemistry, Emory University, Atlanta, Georgia 30322, United States

S Supporting Information

ABSTRACT: Coupled intramolecular and intermolecular vibrational quantum dynamics, using an ab initio potential energy surface, successfully describes the subpicosecond relaxation of the OD and OH stretch fundamental and first overtone of dilute HOD in ice Ih. The calculations indicate that more than one intermolecular mode along with the three intramolecular modes is needed to describe the relaxation, in contrast to a recent study using a phenomenological potential in just two degrees of freedom. Detailed time-dependent relaxation pathways from 6-mode calculations are also given.

The dynamics and spectroscopy of vibrational excitation and relaxation in liquid and solid water are a central research theme in Chemistry, both experimentally[1−13] and theoretically.[14−18] The ability to dope neat water with HOD in dilute amount has opened a window on this research by isolating the excitation and relaxation to this dopant. This had lead to a number of important experimental and theoretical studies of this system in particular.[4−16] Simplified interpretations of HOD vibrational relaxation invoking two modes, e.g., the initially excited OH stretch and the OO stretch in the H-bond network, as described by the phenomenological Lippencott−Schroeder (L-S) potential,[19] have recently been reported in connection with state-of-the-art 3D IR experiments.[13] This simplified description, which was applied successfully, is at odds with the alternate analyses of Rey and Hynes[14,15] and Lawrence and Skinner,[16] albeit in the context of relaxation in the liquid phase. These analyses suggest a more complex relaxation pathway involving intramolecular as well as intermolecular modes. These seminal works invoked perturbative treatments of couplings together with experimental data to obtain relaxation times in reasonable agreement with experiment. Ultrafast resonant vibration-to-vibration (VV) transfer of H_2O in neat water has been investigated using a quantum harmonic model by Poulsen et al.[17]

Given the surprising success of the recent application[13] of the 2-mode L-S potential, we undertook state-of-the-art ab initio quantum calculations of the vibrational relaxation of HOD in ice and present the results here. The calculations are in very good accord with experiment and elucidate the relaxation pathways.

The ab initio approach we take combines the two validated components, namely the potential and the quantum description of the vibrational dynamics. The former is provided by the Wang−Huang−Braams−Bowman (WHBB) potential.[20] This is a high-dimensional, permutationally invariant fit to high-level ab initio intrinsic two- and three-body potentials and a spectroscopically accurate monomer potential. The potential has been used in a variety of quantum vibrational calculations, ranging from a benchmark calculations of the dissociation energy and predissociation dynamics of the water dimer[21,22] and trimer[23,24] to elucidation of the IR spectra of isomers of the water hexamer[25] and in all cases giving unprecedented agreement with experiment. The potential has also been used to obtain the coupled-mode IR spectra of amorphous ice and ice Ih in the bend and OH-stretch regions, using roughly 200 monomers to model the ices.[26] The quantum vibrational dynamics are made feasible by using the local monomer model.[27] In this model the nine normal modes of each monomer in a cluster are obtained, and then the Schroedinger equation is solved in a subset of these modes, but without making any further approximations to the potential (which includes the interaction with all other monomers fixed at their reference configuration). In the applications mentioned above for the IR spectroscopy the three intramolecular modes were considered, and thus the fully coupled Schroedinger equation is formally equivalent to that for a (perturbed) isolated water monomer. This model has been tested for the water dimer and trimer and has been shown to give vibrational energies that are within 15 cm^{-1} or less of benchmark results.[27]

We apply this combined ab initio approach here to study vibrational energy relaxation. We do this considering up to six of the nine local normal modes of one HOD monomer embedded in the ice Ih model of 116 monomers. Virtual-state configuration interaction (VCI) calculations are performed using the code MULTIMODE,[28−30] where the virtual states are eigenfunctions of the ground vibrational-state vibrational self-consistent field Hamiltonian. Details of the calculations are given in the Supporting Information (SI). Note the position of the HOD is the center of the cluster (see SI for more details), and thus the HOD is fully H-bonded. Experimentally there is no such uniquely defined location, of course. We comment on this briefly at the end and describe future work to investigate site inhomogeneity.

First, we present calculated three-(intramolecular)-mode HOD fundamental and overtone OD and OH-stretch excitation energies in the gas phase and in ice Ih, obtained with a small VCI basis of order 729 and compare to experiment

in Table 1. Agreement with experiment for isolated HOD is excellent; this is expected because the monomer potential is, as

Table 1. Energy Differences in cm^{-1} of gas HOD and HOD in Ice Ih from 3-Mode MULTIMODE (MM) Calculations and Experiments

	n_{f-i}	gas MM	gas exp	ice Ih MM	ice Ih 2D-IR[a]
OD(v)	1−0	2723	2724	2419	2415
	2−1	2640	2640	2315	2251[b]
OH(v)	1−0	3707	3707	3270	3279
	2−1	3536		3087	3123[b]

[a]Ref 12. [b]Estimated from the experimental band.

noted above, of spectroscopic accuracy for isolated H$_2$O.[31] Much more significant is the agreement with experiment for the fundamentals of HOD in ice. This level of agreement is further validation of the accuracy of the current approach. Note the large red-shifts (437 and 304 cm^{-1}) from the gas-phase of OH and OD-stretch fundamentals. This is consequence of the strong hydrogen bonding of these modes in the ice environment. It is also important to note that the eigenstates of these fundamentals and overtone states are quite pure in both the gas-phase and 3-mode embedded cases. (The VCI expansion coefficients are given in the SI.)

Having validated the approach for the HOD fundamentals and overtone in ice, the goal is to study the vibrational relaxation. Since it is known experimentally that this relaxation is in the subpicosecond time scale (and clearly does not involve a simple VV resonant relaxation), we reasonably assume, as others have,[12−16] that the relaxation is via coupling to localized intermolecular modes, and so the local monomer description of these modes should be reasonable. The six intermolecular modes along with three intramolecular ones are given in Figure 1, along with the harmonic frequencies. Including all nine
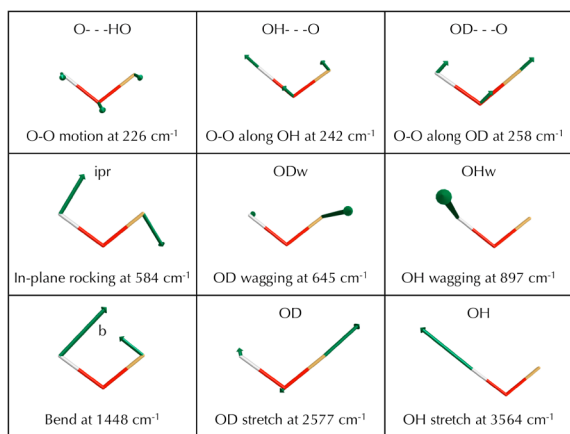

Figure 1. Depiction of all local-normal modes of the HOD monomer in ice environment. Abbreviation at top. Full description and harmonic frequency at bottom.

modes in a fully coupled calculation is too computationally intensive and so proceeded as follows. We began by adding one intermolecular mode at time to the 3-mode calculation and investigated the level of mixing in the eigenstates of the corresponding Hamiltonian. Based on this approach, we found that 6-mode calculations provide reasonably converged results. The 6-mode calculation is done with a 24 199 VCI basis.

Details of the intermolecular mode couplings are presented in the SI.

The wavepacket calculations are straightforward in the basis of eigenstates of the Hamiltonian, once a choice for the wavepacket at $t = 0$ is made. For this a virtual state is selected that represents the OD or OH stretch with fundamental or overtone excitation at 0 K. This nonstationary state is then propagated in the basis of eigenstates. The details are given in the SI.

The dynamics of OD/OH relaxation is characterized by the time-dependent decay of the initial state population. This is shown in Figure 2 for the four initial states of interest. First, note the relaxation occurs in the subpicosecond time frame and that the two overtones relax faster than the corresponding fundamentals. To quantify the relaxation time, we fit the data with mono- and bi- exponential functions, as suggested in previous experiments.[10−12] The fitted lifetimes are summarized in Table 2 and compared with experiments. (Details of data fitting are given in SI.) First, we see the lifetime for the OD and OH fundamentals agree well with both 2D-IR and pump–probe experiments. The lifetime of the OD overtone also agrees well with the recent 3D-IR experiment,[13] which as noted above used the 2-mode L-S model potential in wavepacket calculations to "successfully" capture this rapid decay. A fast relaxation rate on the order of 100 fs is seen for the OH overtone. No direct measurement of this has been performed so far. However, an estimate based on line shape fitting also predicts extremely fast rate.[10]

Also shown in Figure 2 are the populations of initially unpopulated virtual states. The expressions to obtain these are standard and are given in detail in the SI. These are the detailed pathways for the vibrational relaxation. For the OH fundamental, as seen from Figure 2b, the major pathway is $v_{OH} \rightarrow v_{ipr} + 2v_b$ and subsequently to $v_{OD \cdots O} + 3v_{ipr} + v_b$. This short-time decay pathway is in accord with Hynes[14,15] and Skinner,[16] who proposed the relaxation of the OH stretch fundamental to the bend overtone in liquid phase. For the OD fundamental, the dominant relaxing pathway is the high overtone of intermolecular OD wagging mode, as seen from Figure 2a. Clearly other mixed inter and intramolecular states contribute at longer times.

The relaxation pathways for the OD and OH overtones show distinctive features. As seen from Figure 2d, the decay of the OH overtone is strongly correlated with the rise of $2v_b + v_{OH}$ and $v_{OH \cdots O} + 2v_{OH}$. This clearly indicates the mixing of the OH overtone with these two states. For the OD overtone, as shown in Figure 2c, the relaxation is not due to a dominant pathway. This finding is clearly in opposition to the simple 2-mode analysis using the L-S potential, reported by Hamm et al.[13]

To conclude, both intra and intermolecular couplings in HOD are responsible for the vibrational relaxation dynamics of the OH and OD stretch excitations of HOD in ice Ih. The details of the relaxation pathways are, as expected, sensitive to whether the excitation is fundamental or overtone and also specific to OH and OD. Further, it is clear that such complex dynamical process cannot be described by coupling a single OD/OH stretch with a single intermolecular mode, which has been recently suggested in the literature.[12,13] The calculations again demonstrate the accuracy and extendibility of the WHBB water potential and the local monomer quantum dynamical model in the broad research field of the dynamics and spectroscopy of liquid water and ice. Future calculations will address spectral inhomogeneity by considering additional sites
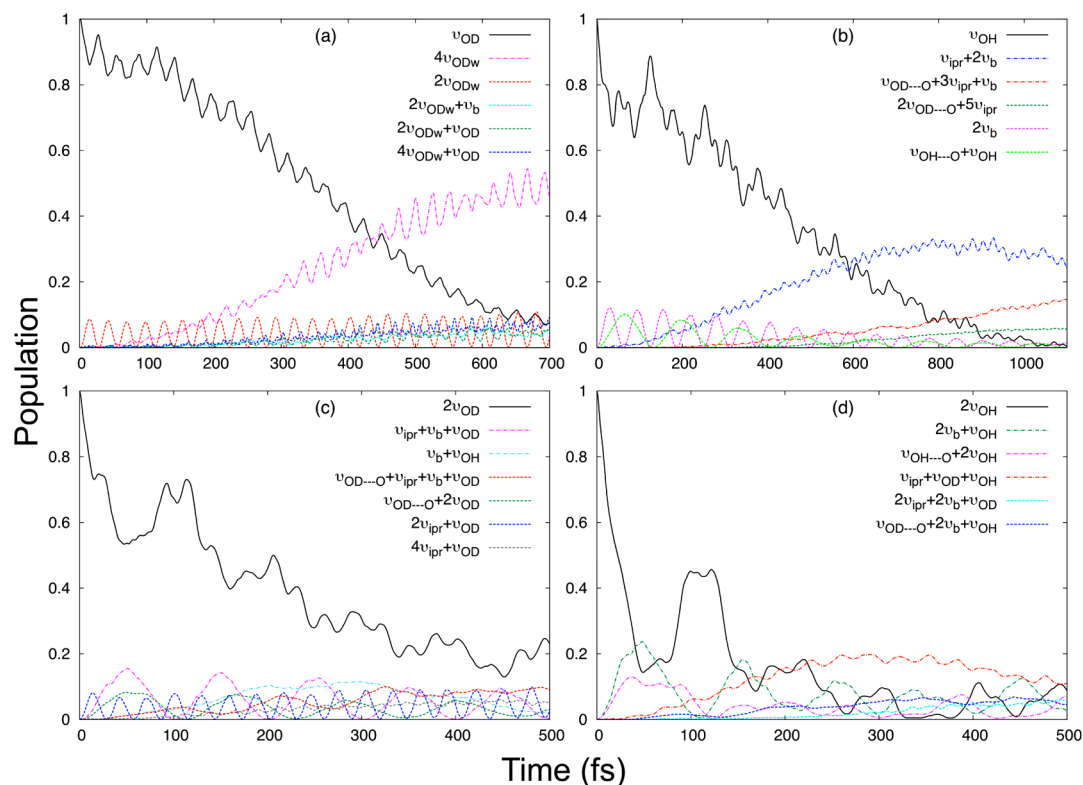
Figure 2. Time-dependent populations of the four excited nonstationary states and major population receivers: (a) OD fundamental, (b) OH fundamental, (c) OD overtone, and (d) OH overtone. Enlarged figures for each panel are given in SI.

Table 2. Lifetime (fs) of OD/OH (v = 1 and 2) from Wavepacket Calculations and Experiments

	n_{f-i}	this work[a]	2D-IR[b]	3D-IR[c]	pump–probe
OD(v)	1–0	422,373	410		480[d]
	2–1	223,296		~200	
OH(v)	1–0	430,447	590		420[e]
	2–1	146,64			20[f]

[a]The two lifetimes at 0 K are obtained by fitting the population decay curves in Figure 2, using both monoexponential and biexponential functions (see SI), respectively. [b]Biexponential fit at 80 K, from ref 12. [c]Estimation at 258 K, from ref 13. [d]Monoexponential fit at 25 K, from ref 11. [e]Monoexponential fit at 180 K from ref 10. [f]From ref 10, an estimated value to fit the transient line shapes.

for HOD. Recent 2D-IR spectra[12] and approximate calculations[32] indicate that this broadening is of the order of 25 cm^{-1}.

ASSOCIATED CONTENT

S Supporting Information

Additional description of theory, data, and analysis are provided in Supporting Information. This material is available free of charge via the Internet at http://pubs.acs.org.

AUTHOR INFORMATION

Corresponding Author

jmbowma@emory.edu

Notes

The authors declare no competing financial interest.

REFERENCES

(1) Vodopyanov, K. L. *J. Chem. Phys.* **1991**, *94*, 5389.
(2) Fecko, C. J.; Eaves, J. D.; Loparo, J. J.; Tokmakoff, A.; Geissler, P. L. *Science* **2003**, *301*, 1698.
(3) Cowan, M. L.; Bruner, B. D.; Huse, N.; Dwyer, J. R.; Chugh, B.; Nibbering, E. T. J.; Elsaesser, T.; Miller, R. J. D. *Nature* **2005**, *434*, 199.
(4) Nibbering, E. T. J.; Elsaesser, T. *Chem. Rev.* **2004**, *104*, 1887.
(5) Woutersen, S.; Emmerichs, U.; Nienhuys, H.-K.; Bakker, H. J. *Phys. Rev. Lett.* **1998**, *81*, 1106−1109.
(6) Gale, G. M.; Gallot, G.; Lascoux, N. *Chem. Phys. Lett.* **1999**, *311*, 123.
(7) Deàk, J. C.; Rhea, S. T.; Iwaki, L. K.; Dlott, D. D. *J. Phys. Chem. A* **2000**, *104*, 4866.
(8) Schwarzer, D.; Lindner, J.; Vohringer, P. *J. Chem. Phys.* **2005**, *123*, 161105.
(9) Seifert, G.; Weidlich, K.; Graener, H. *Phys. Rev. B* **1997**, *56*, R14231.
(10) Dokter, A. M.; Bakker, H. J. *J. Chem. Phys.* **2008**, *128*, 024502.
(11) Smit, W. J.; Bakker, H. J. *J. Chem. Phys.* **2013**, *139*, 204504.
(12) Perakis, F.; Widmer, S.; Hamm, P. *J. Chem. Phys.* **2011**, *134*, 204505.
(13) Perakis, F.; Borek, J. A.; Hamm, P. *J. Chem. Phys.* **2013**, *139*, 014501.
(14) Rey, R.; Hynes, J. T. *J. Chem. Phys.* **1996**, *104*, 2356.
(15) Rey, R.; Møller, K. B.; Hynes, J. T. *Chem. Rev.* **2004**, *104*, 1915.
(16) Lawrence, C. P.; Skinner, J. L. *J. Chem. Phys.* **2002**, *117*, 5827; **2003**, *119*, 1623; **2003**, *119*, 3840.
(17) Poulsen, J. A.; Nyman, G.; Nordholm, S. *J. Phys. Chem. A* **2003**, *107*, 8420.

(18) Bäcktorp, C.; Poulsen, J. A.; Nyman, G. *J. Phys. Chem. A* **2005**, *109*, 3105.

(19) Lippincott, E. R.; Schroeder, R. *J. Chem. Phys.* **1955**, *23*, 1099.

(20) Wang, Y.; Huang, X.; Shepler, B. C.; Braams, B. J.; Bowman, J. M. *J. Chem. Phys.* **2011**, *134*, 094509.

(21) Shank, A.; Wang, Y.; Kaledin, A.; Braams, B. J.; Bowman, J. M. *J. Chem. Phys.* **2009**, *130*, 144314.

(22) Ch'ng, L. C.; Samanta, A. K.; Czakó, G.; Bowman, J. M.; Reisler, H. *J. Am. Chem. Soc.* **2012**, *134*, 15430.

(23) Wang, Y.; Bowman, J. M. *J. Chem. Phys.* **2011**, *135*, 131101.

(24) Ch'ng, L. C.; Samanta, A. K.; Wang, Y.; Bowman, J. M.; Reisler, H. *J. Phys. Chem. A* **2013**, *117*, 7207.

(25) Wang, Y.; Bowman, J. M. *J. Phys. Chem. Lett.* **2013**, *4*, 1104−1108.

(26) Liu, H.; Wang, Y.; Bowman, J. M. *J. Phys. Chem. Lett.* **2012**, *3*, 3671.

(27) Wang, Y.; Bowman, J. M. *J. Chem. Phys.* **2011**, *134*, 154510.

(28) Bowman, J. M.; Carrington, T.; Meyer, H.-D. *Mol. Phys.* **2008**, *106*, 2145.

(29) Carter, S.; Culik, S. J.; Bowman, J. M. *J. Chem. Phys.* **1997**, *107*, 10458.

(30) Bowman, J. M.; Carter, S.; Huang, X. *Int. Rev. Phys. Chem.* **2003**, *22*, 533.

(31) Partridge, H.; Schwenke, D. W. *J. Chem. Phys.* **1997**, *106*, 4618−4639.

(32) Shi, L.; Skinner, J. L. *J. Phys. Chem. B* **2013**, *117*, 15536.